superconductor; ρ suddenly decreases below 5.5 K and tends to zero below 2 K. Nevertheless, the amount of the decrease of ρ is found to depend on the surface state. The sample which is gently rubbed by a soft tissue paper so that it becomes more shiny immediately before mounting on the sample holder, has much smaller decrease of ρ. This is shown for ρ of $Ce(In_{0.5}Sn_{0.5})_3$. Curve A is with this rubbing and curve B is without. Thus we conclude that the superconducting state is not due to bulk sample, but is due to deposits of In–Sn alloy on the sample surface. These deposits are likely to be the eruptions on the sample surface observed by scanning electron microscope. In $Ce(In_{0.3}Sn_{0.7})_3$, the decrease of ρ is clearly seen to have two steps. This is understood because the In–Sn alloy is eutectic and $In_{0.3}Sn_{0.7}$ consists of two components with different compositions and with different superconducting temperatures. The values of these two temperatures are near to those reported [2] on In–Sn alloys, and prove a small amount of this alloys actually deposited on sample surface.

1 G. K. Shenoy, B. D. Dunlap, G. M. Kalvius, A. M. Toxen and R. J. Gambino, *J. Appl. Phys., 41* (1970) 1317.
2 S. C. Harris, *Proc. Roy. Soc. London A, 350* (1976) 267.

D12

A New Family of Sheet Structures: the Oxyselenides Formed by a Rare Earth and a Second Metal

S. BÉNAZETH, J. FLAHAUT*, M. GUITTARD and P. LARUELLE

Laboratoire de Chimie Minérale Structurale associé au CNRS, Faculté de Pharmacie, 4, avenue de l'Observatoire, F75270 Paris Cédex 06, France

Sheet structures are observed in oxyselenides formed by La and a second metal of the IIIA–VA groups of the periodical classification.

$\left.\begin{array}{l}(LaO)GaSe_2\\(LaO)InSe_2\end{array}\right\}$ orthorhombic pseudo tetragonal cells of the $(LaO)GaSe_2$ type

$(LaO)_4Ge_{1.5}Se_5$: orthorhombic cell of the $(NdO)_4$-Ga_2S_5 type, with disordered arrangement of Ge atoms on the Ga sites.

$(LaO)_2SnSe_3$: orthorhombic pseudo tetragonal cell of the $(LaO)_2SnS_3$ type.

$(LaO)SbSe_2$: tetragonal cell of the $(CeO)BiS_2$ type.

All these structures are formed by alternating (LaO) sheets and (M_xSe_y) sheets (M = second metal). The (LaO) sheets are formed by La_4O tetrahedra which share 4 of their 6 edges in a tetragonal or pseudo tetragonal arrangement. The (M_xSe_y) sheets are formed by 2, 3 or 4 layers of Se atoms. The M atoms are only bonded to Se atoms, in octahedral (Sb) or tetrahedral (Ga, In, Ge, Sn) arrangements. Similar compounds are not obtained with the other rare earths. The structure of $(LaO)GaSe_2$, which is only observed with selenides, is described: the cell is orthorhombic space group $P2_1ab$; $a = 5.951(3)$; $b = 5.963(3)$; $c = 12.256(7)$ Å; $Z = 4$; $d_x = 5.84$ Mg m^{-3}; M (MoKα) = 31.3 mm^{-1}.

The structure was established on single crystal data and refined by a least-squares procedure; the final R value is 0.07 on 523 independent reflections. The structure is formed by alternating (LaO) and $(GaSe_2)$ layers, parallel to the (001) plane.

D13

Lanthanide Oxides: Effect of CO_2 on the Yb_2O_3 Hydration

I. CARRIZOSA, J. A. ODRIOZOLA, J. M. TRILLO

Inorganic Chemistry Department, Faculty of Pharmacy, University of Seville, Seville, Spain

and M. F. EBEL

Institut fur Angewandte und Technische Physik. Technische Universität Wien, Vienna, Austria

Recent results in our laboratory [1, 2] have proved that the heaviest terms of the 4f series oxides undergo bulk hydration and carbonation when exposed to the atmospheric air, in contradiction with the previous literature [3]. The main difference between the lighter and the heavier 4f oxides is related to kinetic aspects.

In the case of the hydration of the La_2O_3, Rosynek [4] has shown a certain inhibition effect exerted by the CO_2. In the present paper, the interaction of the Yb_2O_3 with H_2O, H_2O/CO_2 mixtures and atmospheric air has been examined through XPS and TPD measurements. The effect of CO_2 on the hydration of ytterbium sesquioxide is discussed in the light of those results.

Ytterbium hydroxycarbonate was precipitated with NH_3 from nitrate solutions. Yb_2O_3 was finally prepared by calcining the precipitate in air at 873 K. The sample here studied was characterized by X-ray diffraction, thermogravimetric (TG) and differential thermal analyses (DTA), IR spectroscopy and pore size distribution. Data about preparation and characterization are reported in [1].

Details concerning the temperature programmed decomposition (TPD) device are given in [5]. All the experiments were carried out in helium flow (30 ml min^{-1}) at a heating rate of 8 K min^{-1}. The XPS analyses were performed using a KRATOS XSAM 800 (Mg K$_\alpha$, radiation, 15 kV, 10 mA, vacuum better than 1 X 10^{-8} torr).

Figure 1 shows characteristic TPD traces for water elimination from Yb_2O_3 samples previously activated at 1173 K, then hydrated and finally evacuated 30 min at 330 K, all the processes being carried out in the TPD system. The TPD trace (a) corresponds to a sample aged in air for 10 days, no change is observable for aging periods from a few hours to several days. The maximum at 440 K can be ascribed to vicinal OH^- elimination and the long tail at higher temperatures to isolated OH^-. Integration of the TPD trace leads to a coverage of 8 molec/nm^2, which is in the range of a surface process. According to [6], a water monolayer is completed with 7.9 molec/nm^2. A similar trace is encountered in (b) for an Yb_2O_3 sample exposed to a mixture of H_2O at a partial pressure of 15 torr and CO_2 at 2.4 torr, with a calculated H_2O coverage of 3.5 molec/nm^2. It is noteworthy that the CO_2 pressure is considerably higher than that corresponding to the atmospheric air (0.3 torr). In both (a) and (b) experiments, small amounts of CO_2 evolve together with the water. For comparative purposes the dashed line (c) belongs to an activated Yb_2O_3 in the same conditions and exposed 24 hours to a decarbonated H_2O pressure of 15 torr and at 298 K. The water amount is now 17.1 molec/nm^2 which largely exceeds the surface capacity and lends support to a bulk hydration at an appreciable rate.

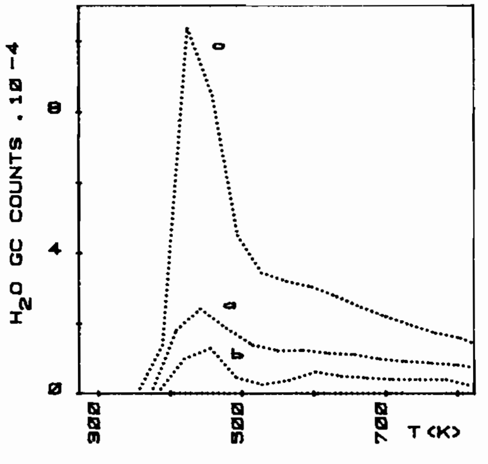

Fig. 1. TPD traces for H_2O elimination from Yb_2O_3 activated at 1173 K.

The results of (a) and (b) are in agreement with XPS data shown in Fig. 2 for O(1s) binding energy of 530.4 and 532.0 eV, corresponding to oxide and hydroxyl species respectively. With the time of exposure to the air of an Yb_2O_3 sample evacuated at 1173 K, a shoulder corresponding to the first stage of hydration emerges and increases, becoming a peak, (e), after 46 hours and then slowly changing over long periods up to 2000 hours. According to Padalia *et al.* [7], this behaviour can be ascribed to a surface process giving an OH^- monolayer on the oxide surface. It agrees with TPD data for the same periods of time, corresponding to a surface reaction. The simultaneous presence of hydroxyl and carbonate species, which are not discriminated in our spectra, is the reason for intensity ratios bigger than in Padalia's experiments. From the above mentioned results it can be deduced that the presence of CO_2 avoids the possibility of a fast bulk hydration and a surface adsorption is only obtained.

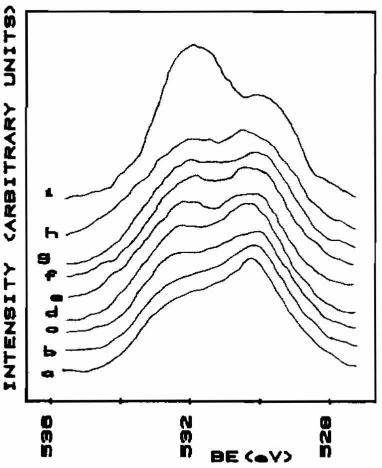

Fig. 2. O(1s) XPS spectra of Yb_2O_3 samples aged in air for: a) fresh sample; b) 1 hour; c) 2 hours; d) 21 hours; e) 46 hours; f) 68 hours; g) 99 hours; h) 2153 hours, and i) 4 years, datum from ref. 1.

For a period of exposure to the air of 4 years, Fig. 3, the uptake of H_2O and CO_2 is large. Integration of TPD traces gives H_2O and CO_2 amounts that

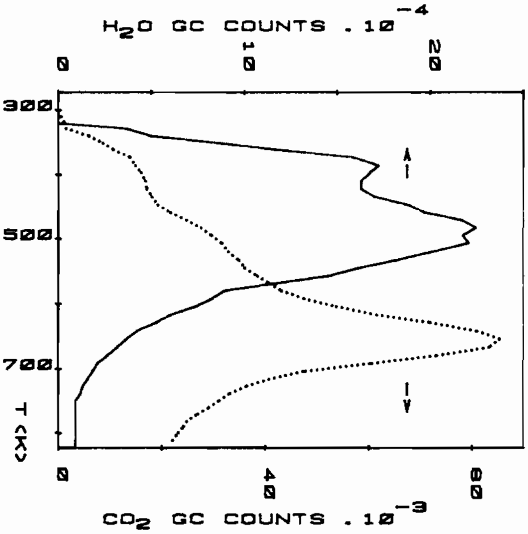

Fig. 3. TPD of Yb_2O_3 aged in air for 4 years.

largely exceed a surface process and can be ascribed to a hydroxycarbonate phase. In addition, curve (i) of Fig. 2 shows the XPS spectra of Yb_2O_3 aged for 4 years in air. As can be observed, the ratio of hydroxyl signal intensity to the one of the oxide clearly shows that most of the oxygens within the photoelectron escape depth are in the form of OH^- group.

Although the mechanistic aspects of the slow hydration and carbonation of the heavier Ln_2O_3 are out of the scope of this article, the poisoning effect of CO_2 can be easily understood: CO_2 competes with H_2O for the basic centres necessary for dissociative adsorption. This fact, together with the strongly basic properties of the carbonate and bicarbonate surface species formed on CO_2 adsorption, can hinder the proton mobility.

1 R. Alvero, S. Bernal, J. A. Odriozola and J. M. Trillo; *J. Chem. Soc. Dalton*, in press.
2 R. Alvero, S. Bernal, I. Carrizosa, J. A. Odriozola and J. M. Trillo, *J. Less Comm. Met.*, in press.
3 D. Touret and F. Queyroux, *Rev. Chim. Miner.*, *9*, 883 (1972).
4 M. A. Rosynek and D. T. Magnuson, *J. Catal.*, *46*, 402 (1977).
5 S. Bernal, R. Garcia and J. M. Trillo, *React. Kinet. Catal. Lett.*, *10*, 125 (1979).
6 S. Bernal, R. Garcia, J. M. Lopez and J. M. Rodriguez-Izquierdo, *Collect. Czech. Chem. Comm.*, in press.
7 B. P. Padalia, J. K. Gimzewski, S. Affrossman, W. C. Lang, L. M. Watson and D. J. Fabian, *Surf. Sci.*, *61*, 468 (1976).

D14

Preparation of Actinide Thin Film Deposits for Nuclear Physics and Solid State Physics Researches

J. KWINTA*, PH. BROSSARD, J. J. MICHEL and J. THOREUX

Commisariat à l'Energie Atomique, Centre d'Etudes de Bruyères-le-Chatel, B.P. 561, 92542 Montrouge Cédex, France

Actinide targets used in nuclear physics as well as some samples studied in solid state physics must, generally, meet very precise specifications which determine the quality of the results. This is particularly true for thin film deposits for which the usual characteristics are the following:

Elements: Th, Pa, U, Np, Pu, Am, Cm, Cf...
Chemical state: metal, oxide or salt
Deposit area: $1-10\ cm^2$
Thickness: $10-100\ \mu g\ cm^{-2}$
Homogeneity: better than 10%
Amount of material used: a few milligrams or less

One has also to take into account the radioactivity of the actinides (especially the short half life ones) and the fact that some isotopes are scarce.

These restrictions impose to set up special equipments in glove boxes for the deposition and the control. The examples of electrospraying and focused ion beam sputtering are presented. Although the electrodeposition in aqueous or organic media and the classical vacuum deposition are widely used, these techniques will not be discussed in this paper.

Electrospraying. The principles of electrospraying were first stated by Zeleny in 1917 [1]. However the technique only became efficient after the work of Verdingh and Lauer at the CBNM (GEEl, Belgium) [2]. A solution containing the element to be deposited flows through a capillary. A positive potential with respect to the substrate is applied to a wire lodged into the capillary. At its exit, due to the electrical forces, the drop becomes unstable and explodes forming a spray which sprinkles the substrate. Usually the solvent evaporates before the microdroplets reach the backing. Moreover the electrical field accelerates the formed particles improving their adhesion on the foil. For example, in the case of actinide acetates dissolved in methanol and with usual experimental conditions, the number of such droplets is about 4×10^{11} per cubic centimeter. A special mechanism allows the substrates to move in x and y directions in order to improve the film uniformity. The deposits can be heated at 450 °C to get the oxides. The whole system can easily be mounted in a glove box with exterior monitoring. We have realized in our laboratory targets or samples of the following isotopes: ^{230,232}Th, ^{231}Pa, ^{237}Np, ^{233,235,238}U, ^{239,241}Pu, ^{241,243}Am, ^{244}Cm, ^{252}Cf as acetates or oxides.

Focused Ion Beam Sputtering

One drawback of electrospraying is that only a limited number of chemical species can be deposited *i.e.* mainly acetates and eventually oxides. Thus focused ion beam sputtering was developed in our laboratory for actinide target preparations as this technique allows the use of only milligrams of starting material. Moreover practically all the chemical forms of actinide compounds, including the metals, can be sputtered. The principle is the following: ions (generally from rare gas) produced by an ion source (duoplasmatron-type or cold cathode-type) are accelerated and then focused by mean of einzel lens on the source material. The sputtered atoms are then collected on the substrates suitably disposed around the beam-stop.

The typical running parameters are the following:
– ion current: 1–2 mA
– extraction voltage: 10 kV
– focus voltage: 1–2 kV